Networkmetrics: Multivariate Visual Analytics for Time Series Networking Data

José Camacho

Dpt. of Signal Theory, Telematics and Communications
ETSIIT - CITIC - University of Granada (Spain)

Abstract

This report presents a framework for time series data analysis with application to networking data. The framework combines the powerful analysis capabilities of multivariate models based on projection subspaces with the benefits of data visualization. The approach is based on a recently proposed framework for Exploratory Data Analysis (EDA), which main goal is the knowledge generation. This is tackled using a number of appropriate techniques to maximize insight into a data set and uncover the underlying structure, including the identification of relevant features and abnormal observations. A number of examples are presented to motivate the use of the EDA framework. Results show that with only a few plots correctly interpreted, the user gains a detailed insight into the data, including valuable information for data modelling and decision making.

Keywords: Multivariate Analysis, Latent Structures, Exploratory Data Analysis, Traffic Analysis, Time Series, Visual Analytics

1. Introduction

Network traffic analysis is a field of constant evolution as a consequence of the evolution of the communication systems and protocols. In this changing context, traffic monitoring is an issue of great concern in order to understand and optimize the telecommunication technologies [1, 2]. The successful monitoring of networking data sets requires the parsing and analysis online of tons of time series data. There is a clear interest in developing methods to manage these scales of data while taking advantage of *the basic importance of simply looking at data* [3]. This interest has lead to the development of sophisticated visualization tools within the so-called visual analytics research area [4]. After all, *a picture is worth a thousand log entries* [5].

The present work proposes the application of Exploratory Data Analysis (EDA) based on multivariate models to the analysis of networking data. EDA has been employed for decades in many research fields, including social sciences, psychology, education, medicine, chemometrics and related fields [6] [7]. EDA is both a data analysis philosophy and a set of tools [3], which main goal is to identify patterns in the data in order to extract information out of complex data sets. Nevertheless, while the philosophy has essentially remained the same, the tools are in constant evolution, as numerous recent references suggest [8] [9] [10] [11]. This is the direct consequence of the increasing complexity of the problems tackled with data analysis methods thanks to increasing computers capabilities. Specially challenging is the continuously growing size of the data sets, the so called Big Data problem. Networking data sets are a main example of such problem.

In high dimension data sets, with a large number of features, projection models based on latent structures are valuable tools within EDA. Standard projection models are Principal Component Analysis (PCA) [12] [13] [6] and Partial Least Squares (PLS) [14] [15] [16]. These models and the set of tools used in combination [17] [18] [19] [20] simplify the visual analysis of complex data sets, pointing out to especial observations (outliers), clusters of similar observations, groups of related features, and crossed relationships between specific observations and features. Furthermore, there is a vast literature on missing data estimation [21] [22] [23], data fusion [24] [25], hypothesis testing [26] [27] [28], data equalization [29] [30] [31], data preprocessing [32] and other data analysis procedures concerning projection models. All these methods conform a powerful tool set for EDA that provides the analyst with high

Email address: josecamacho@ugr.es, pablopadilla@ugr.es, jedv@ugr.es (José Camacho)

capabilities.

Such a powerful tool set is of interest to analyze any type of data, including networking data. Unfortunately, the extension of projection models to typical time series data mining problems, such as traffic data analysis, has been very limited. The aim of this paper is to extend the visual tools within the EDA approach based on projection subspaces for its efficient application in very large, times series, data sets. In particular, the contribution of the paper is two-fold:

- To introduce a methodology and a set of tools [33] for data interpretation to the networking community. The framework presented is a combination of techniques, some of which are already well known while some others are recent [17, 34].
- To present the extension of these methods to large scale, time series data. In particular, the main contributions at this point is the development of the compressed score plots (CSPs) using Exponentially Weighted Moving Average (EWMA) clustering. This contribution is paramount to handle large amounts of data while retaining the visualization capability of the tools in the framework.

Because this paper presents an extension of techniques with an important impact in research areas such as chemometrics and psychometrics to networking data, the approach is named networkmetrics.

The paper is organized as follows. Section 2 discusses related work on the topic. Section 3 introduces projection models. Section 4 reviews the framework for EDA based on projection models. Section 5 motivates the use of this framework on three simple data sets related to networking with a reduced number of observations but many variables. In Section 6, the concluding remarks are drawn.

2. Related Work

The growing interest in network traffic analysis is evidenced by specific network traffic symposia, such as the *Traffic Monitoring and Analysis (TMA)* [35]; the *Passive and Active Measurement (PAM) Conference*; the *International Workshop on Traffic Analysis and Classification (TRAC)* [36] that is part of the *International Wireless Communications and Mobile Computing (IWCMC)*; and the *Large Scale Network Analysis (LSNA)* [37], part of the *World Wide Web (WWW) congress* and the *Internet Measurement Conference (IMC)* [38].

Reference [5] reviews the different sources of data for network monitoring for security, the design principles for visual tools and the open source tools available in the market. Although the visual analytics theory has been embraced by the network analysis field, see for instance [39, 40, 41, 42], there is a lack of powerful data analysis methods. In particular, network analysis is typically limited to univariate or low dimension time series signals [5]. Multivariate techniques have been mainly applied to anomaly detection [43, 44, 45, 46]. However, the most suited application of these techniques is data analysis, with the goal of data understanding. Additionally, visual techniques are very specific for a type of data, such as NetFlow data [47], traffic data [48], etc.

This paper introduces powerful analysis methods to treat and visualize highly multivariate data sets without assumptions on the data source. That is, the approach is context free. The methods are extended to large, time series, data sets that make them specially suited to networking data, filling the gap of the other visualization techniques.

3. Multivariate Techniques based on Projection Subspaces

Multivariate techniques based on projection subspaces are typically applied to two-way data sets, although extensions of these models to multi-way data sets also exist [49]. Most of the data collected in a problem domain can be parsed into a two-way data set, where a number of variables or features (columns) are measured/computed for a number of observations or objects (rows). For instance, traffic data analysis can be performed by computing, for each single flow, a number of features such as mean packet and payload size, protocol, flags, etc [50]. The result can be stored in a two-way matrix where the columns are the different features and the rows represent the flows. By applying a multivariate technique to this matrix, the network manager may find the patterns in the traffic of the network.

Both PCA and PLS are two-way methods that perform a similar solution to the same problem: data collinearity in highly multidimensional data sets. Data collinearity refers to high correlation among the data variables or features. Data understanding is subject to identifying collinearity, since the latter is found when the true, latent, dimension of the data is much lower than the actual number of features. For instance, the time-series traffic load in the several routers in the path of a Denial of Service (DoS) attack may be statistically correlated. Multivariate techniques may help to eluci-

date this, showing that there is a single main source of traffic data.

The approach of PCA and PLS to overcome the problems derived from collinearity is to identify a reduced number of new features, referred to as latent variables (LVs) or specifically in PCA as principal components (PCs). These LVs are obtained as a combination of the original features in the data. In standard PCA and PLS, the LVs are linear combinations of the original features, but non-linear extensions also exist [51]. For a given data set, the LVs are found by maximizing a given quadratic function, variance in the case of PCA and covariance for PLS. The operation to obtain the LVs from the original features can be geometrically interpreted as a projection operation. Thus, projection models can be understood as projection subspaces of the original feature space.

3.1. Unsupervised analysis: PCA

The aim of PCA is to find the subspace of maximum variance in the M-dimensional feature space using a $N \times M$ calibration matrix $\mathbf{X}$. The original features, commonly correlated, are linearly transformed into a lower number of uncorrelated features: the PCs. The directions of the PCs are obtained from the eigenvectors of $\mathbf{X}^T \cdot \mathbf{X}$, typically for mean centered $\mathbf{X}$. Also, $\mathbf{X}$ may be scaled so that all variables have an adequate load on the final model. Without additional assumptions, the autoscaling operation, where all variables are centered and scaled to unit variance, is commonly used.

PCA follows the expression:

$$\mathbf{X} = \mathbf{T}_A \cdot \mathbf{P}_A^t + \mathbf{E}_A, \tag{1}$$

where $\mathbf{T}_A$ is the $N \times A$ score matrix containing the projection of the observations in the A PCs sub-space, $\mathbf{P}_A$ is the $M \times A$ loading matrix containing the A eigenvectors of $\mathbf{X}^T \cdot \mathbf{X}$ with highest eigenvalues associated and $\mathbf{E}_A$ is the $N \times M$ matrix of residuals. The number of PCs retained in a PCA model, A, is a principal choice [13] [52], which in general can be regarded as an application dependent decision [53]. When no dimension reduction is done, that is $A = Rank(\mathbf{X})$, PCA is just a rotation of the axes.

PCA is suited for applications in which there is interest in splitting variance in typically two orthogonal sub-spaces: the structure or model subspace and the residual subspace. Examples of such applications are dimensionality reduction [54] [55] [56] [57] and process monitoring [58] [59]. In particular, in the context of data mining, PCA has been typically regarded as a simple preprocessing tool for dimensionality reduction. This is particularly appropriate when $\mathbf{X}$ contains highly collinear data, so that several eigenvalues in $\mathbf{X}^T \cdot \mathbf{X}$ are low enough to be considered as noise. However, in the context of EDA, PCA is a principal technique, and the information from each subspace (residual and model subspaces) may be interpreted together.

3.2. Supervised analysis: PLS

PLS essentially performs an alternative solution of the linear regression problem to the least squares solution. The linear regression problem is defined by the following expression:

$$\mathbf{Y} = \mathbf{X} \cdot \mathbf{B} + \mathbf{F} \tag{2}$$

where $\mathbf{Y}$ is the $N \times K$ matrix of features that are to be estimated, $\mathbf{X}$ is the $N \times M$ matrix of features available to estimate $\mathbf{Y}$, $\mathbf{B}$ is the $M \times K$ matrix of regression coefficients and $\mathbf{F}$ is the $N \times K$ matrix of residuals. A possible way to interpret $\mathbf{B}$ is as a model of $\mathbf{Y}$, being $\mathbf{X}$ the input of the model.

Ordinary Least Squares (OLS) or simply least squares performs a solution to the linear regression problem that minimizes the quadratic error. The least squares solution for (2) is:

$$\hat{\mathbf{B}}_{LS} = (\mathbf{X}^T \cdot \mathbf{X})^{-1} \cdot \mathbf{X}^T \cdot \mathbf{Y} \tag{3}$$

The inversion of the matrix $\mathbf{X}^T \cdot \mathbf{X}$ requires it to be non-singular. Moreover, the OLS solution is highly unstable, leading to a poor estimation performance when this matrix is ill-conditioned. The good conditioning of such a matrix is dependent on the degree of independence among features in $\mathbf{X}$. Therefore, if the features of $\mathbf{X}$ are highly collinear, the estimation of $\mathbf{Y}$ should not be performed directly from $\mathbf{X}$.

An alternative is to predict $\mathbf{Y}$ from the LVs in $\mathbf{X}$. The aim of the PLS regression is to estimate $\mathbf{Y}$ from the subspace of $\mathbf{X}$ that maximizes its covariance with $\mathbf{Y}$. The partial linear regression problem between normalized matrices $\mathbf{X}$ and $\mathbf{Y}$ can be stated as:

$$\begin{aligned} \mathbf{X} &= \mathbf{T}_A \cdot \mathbf{P}_A^T + \mathbf{E}_A \\ \mathbf{Y} &= \mathbf{T}_A \cdot \mathbf{Q}_A^T + \mathbf{F}_A \end{aligned} \tag{4}$$

where $\mathbf{T}_A$ is the $N \times A$ score matrix that contains the projections of $\mathbf{X}$ to the latent A-dimensional subspace, $\mathbf{P}_A$ and $\mathbf{Q}_A$ are the $M \times A$ and $K \times A$ regressor matrices, also called loading matrices, and $\mathbf{E}_A$ and $\mathbf{F}_A$ are the $N \times M$ and $N \times K$ matrices of residuals of $\mathbf{X}$ and $\mathbf{Y}$, respectively. Equation (4) can be rearranged in the following form:

$$\mathbf{Y} = \mathbf{X} \cdot \mathbf{R}_A \cdot \mathbf{Q}_A^T + \mathbf{F} \tag{5}$$

with:

$$\mathbf{R}_A = \mathbf{W}_A \cdot (\mathbf{P}_A^T \cdot \mathbf{W}_A)^{-1} \quad (6)$$

where $\mathbf{W}_A$ is a $M \times A$ matrix of weights. Thus, a PLS model is represented by matrices $\mathbf{P}_A$, $\mathbf{W}_A$ and $\mathbf{Q}_A$.

A variant of PLS for supervised classification is PLS-Discriminant Analysis (PLS-DA) [60]. In PLS-DA, matrix $\mathbf{Y}$ is artificially generated with dummy variables, which codify the different classes in the data set. Typically, $\mathbf{Y}$ is constructed with as many features as classes. All the observations belonging to a class have value 1 for the corresponding feature, and -1 for the rest. This PLS variant is especially useful in the context of data classification, as it will be shown later on in this paper.

Like in PCA, it is customary to mean-center and scale variables in both $\mathbf{X}$ and $\mathbf{Y}$ blocks.

4. Exploratory Data analysis

In EDA, PCA and PLS can be used to improve the understanding of a two-way data set, with a number of observations of a number of features, mainly in the following three main aspects:

a) The distribution of the observations, e.g. the distribution of the flows in a traffic data set. This distribution, in particular the existence of outliers and clusters, contains relevant information for data understanding. Thus, outliers represent abnormal situations that may be very informative in certain contexts. Clusters of observations may represent habitual situations. The separation among clusters may reflect different operation points in the phenomenon of interest. Periodical switching among clusters may reflect repetitive patterns.

   Data sets with several tens of features are common in many areas related to networking, for instance in anomaly detection [45] or traffic classification [61]. Because of the dimension of the data, the direct observation of data distribution in these data sets is not possible, and the visualization of selective pairs of features at a time is a tedious approach. PCA and PLS can be used straightforwardly to visualize the distribution of the data in the latent subspace, considering only a few LVs that contain most of the variability of interest. Score plots [13] are used for this purpose.

b) The relationships among features, e.g. is it the mean size of a packet related to the length of the flow?. PCA or PLS can be used to find relationships among features. Traditionally, Factor Analysis (FA) [6] [13] was used for this purpose. Nevertheless, the combination of PCA and PLS projection models with a recent method termed Missing Data Methods for Exploratory Data Analysis (MEDA) [17] outperforms traditional FA techniques. Also, loading plots [13] are useful to investigate the distribution of the features.

c) The connection between observations and features. The investigation of the connection between observations (e.g. P2P flows) and features (e.g. high mean packet size) in the latent subspace is principal to gain a complete picture of the data, for instance to unveil potential causes for the apparition of outliers and clusters. Traditionally, biplots [18] have been used for this purpose. Also, an extension of MEDA named observation-based MEDA or *o*MEDA [34], is useful in this context.

4.1. Score plots

When a projection model is calibrated, no matter the purpose, the distribution of the scores should always be inspected. This is a common flaw in research papers that use PCA for dimension reduction. The distribution of the scores has to be inspected to detect potential artifacts, such as outliers, that may render the dimension reduction inappropriate. The same model (same covariance structure) may be the result of very different data distributions. For instance, in Figure 1, the score plots of three completely different data distributions that provide exactly the same PCA model are shown: a multinormal distribution, a distribution with one outlier and a distribution with two clusters[1]. This example illustrates that the success of the application of projection models requires the correct interpretation of the distribution of the observations. For instance, for dimension reduction, outliers should be isolated from the rest of the data and the model subspace recomputed. Also, for EDA, the three plots represent a very different situation. Coming back to the traffic data example, the first plot represents a normal distribution of flows, the second plot highlights a special traffic flow which could be a network attack, and the third plot shows two differentiated types of traffic, which could be P2P and client-server traffic. Therefore, the inspection of score plots or equivalent tools is strongly recommended.

[1] The ADICOV algorithm [62] was employed to simulate these data sets.

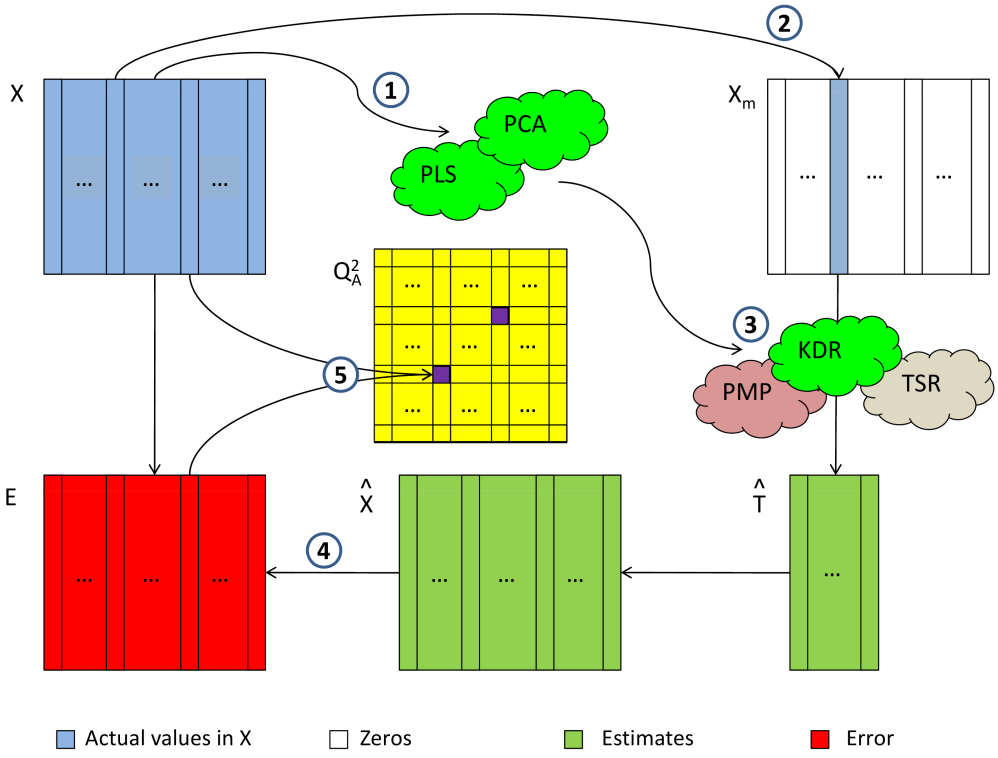

Figure 2: MEDA technique: (1) model calibration: a PCA or PLS model is computed from X; (2) introduction of missing data: to build $\mathbf{X}_m$, all columns in $\mathbf{X}$ except m are filled with zeros; (3) missing data imputation using an algorithm such as Known Data Regression (KDR), Projection to Model Plane (PMP) or Trimmed Score Regression (TSR) [21, 22]; (4) error computation from actual data and estimates; (5) computation of matrix $\mathbf{Q}^2_A$.

4.2. MEDA

MEDA [17] is a tool to find the relationships among the features in the data. It can be applied in any subspace of interest, including PCA and PLS. The MEDA approach is depicted in Figure 2. Firstly, a projection model is fitted from the calibration $N \times M$ matrix $\mathbf{X}$ (and optionally $\mathbf{Y}$). Then, for each feature m, matrix $\mathbf{X}_m$ is constructed, which is a $N \times M$ matrix full with zeros except in the m-th column where it contains the m-th column of matrix $\mathbf{X}$. Using $\mathbf{X}_m$ and the model, the scores are estimated with a missing data method. The known data regression (KDR) method [21, 22] is suggested at this point. From the scores, the original data is reconstructed and the estimation error computed. The sum of squares of the estimation error is compared to that of the original data according to the following index of goodness of prediction:

$$q^2_{A,(m,l)} = 1 - \frac{||\hat{\mathbf{e}}_{A,(l)}||^2}{||\mathbf{x}_{(l)}||^2}, \quad \forall l \neq m. \tag{7}$$

where $\hat{\mathbf{e}}_{A,(l)}$ corresponds to the estimation error for the l-th feature using a model with A LVs and $\mathbf{x}_{(l)}$ is its actual value. The closer the value of the index is to 1, the more related features m and l are. After all the indices corresponding to each pair of features are computed, matrix $\mathbf{Q}^2_A$ is formed so that $q^2_{A,(m,l)}$ is located at row m and column l. This matrix is similar in nature to a element-wise squared correlation matrix, but with better capabilities to distinguish between structure and noise [17]. More details on MEDA can be found on [17] and [33].

For interpretation, when the number of features is large, MEDA can be used in combination with loading plots, which are similar to score plots and show the distribution of the features in the model subspace.

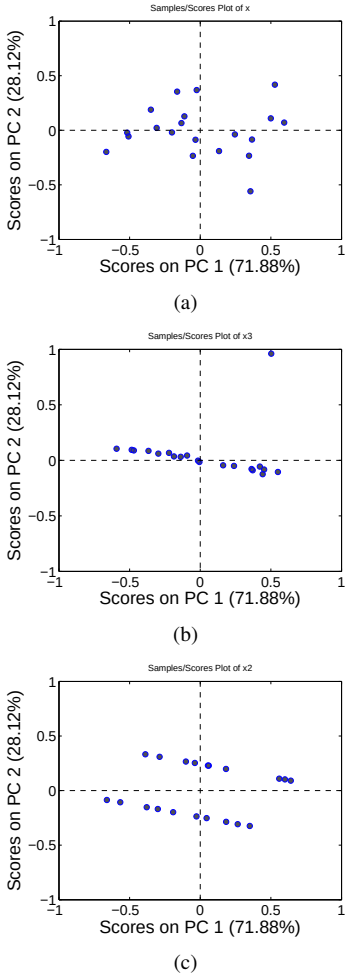

Figure 1: Three different scores distributions for the same PCA model with 2 PCs.

4.3. o*MEDA*

*o*MEDA [34] is a variant of MEDA to connect observations and features. Basically, *o*MEDA is a MEDA algorithm applied over a combination of the original data and a dummy variable designed to cover the observations of interest. Take the following example: a number of subsets of observations (e.g. traffic flows) $\{\mathbf{C}_1, ..., \mathbf{C}_N\}$ form different clusters in the scores plot that are located far from the bulk of the data, $\mathbf{L}$. One may be interested in identifying, for instance, the features related to the deviation of $\mathbf{C}_1$ from $\mathbf{L}$ without considering the rest of clusters. For that, a dummy variable $\mathbf{d}$ is created so that observations in $\mathbf{C}_1$ are set to 1, observations in $\mathbf{L}$ are set to -1, while the remaining observations are left to 0. Also, values (weights) other than 1 and -1 can be included in the dummy variable if desired. *o*MEDA is then performed using this dummy variable.

The *o*MEDA technique works as follows. Firstly, the dummy variable is designed to cover a subset of observations and combined with the data set. Then, a MEDA run is performed by predicting the original features from the dummy variable. The result is a single vector, $\mathbf{d}_A^2$, of dimension $M \times 1$, being M the number of original variables. Values of high magnitude in $\mathbf{d}_A^2$ identify those features related to the deviation among the observations of interest. Also, control limits based on resampling techniques [63] [64] can be obtained. Being $\mathbf{d}$ the dummy variable, the *o*MEDA index follows:

$$d^2_{A,(l)} = \|\mathbf{x}^d_{(l)}\|^2 - \|\hat{\mathbf{e}}^d_{A,(l)}\|^2, \quad \forall l. \tag{8}$$

where $\mathbf{x}^d_{(l)}$ represents the values of the l-th variable in the original observations different to 0 in $\mathbf{d}$ and $\hat{\mathbf{e}}^d_{A,(l)}$ is the corresponding estimation error. For a deeper description of the *o*MEDA algorithm refer to [34]. More details on *o*MEDA can also be found on [33].

5. EDA in networking data sets of reduced size

This section motivates the use of the EDA framework presented here in networking data sets. It will be shown that the framework can be equally applied to very different data sets, with similar or improved capabilities in comparison with context specific approaches. The obvious benefit is that the IT manager or IT analyst only needs to learn the use of a single visualization approach for handling a wide variety of problems and situations.

5.1. Low-size traffic analysis

The next example illustrates the use of the EDA methodology in the context of traffic analysis [65]. The data analyzed were captured in the Networking Laboratory during a 2 hours laboratory session of the course 'Network Management', in the Telecommunications degree of the University of Granada. During this session, the students were dealing with the configuration of polling and traps generation with the Simple Network Management Protocol (SNMP), in the Cisco routers and switches of the laboratory.

The Networking Laboratory consists of 24 user work stations (noted Px) connected to the different networks configured in the laboratory. These 24 work stations are arranged in cells of 4 stations each. The six cells in the laboratory, numbered from 1 to 6, are able to work autonomously from the rest of the cells. Each cell is composed by 4 work stations (Px/1, Px/2, Px/3 and Px/4, where x stands for the cell number) with three network interfaces each one, connected to three different

networks containing a variety of network devices such as three Cisco 1841 routers (Rx-A, Rx-B and Rx-C) and three Catalyst 2950 switches (SWx-A, SWx-B and SWx-C), among others (ATM, Frame Relay and X.25 devices, PBX, etc.).

During part of the laboratory session, SNMP information was acquired from the switches in one of the cells (cell 4) with a one minute sampling interval. The data, acquired with the *snmpwalk* command of the Net-SNMP distribution, were the input and output traffic octets in the 14 interfaces of the three switches. During the session there were two students working in the cell: student 1, located in P4/1, was configuring the SW4-A by means of a Telnet connection, while student 2, located in P4/2, was configuring R4-A, also with a Telnet connection. In addition, during some time intervals in the session, a Neptune attack (SYN flooding) to SW4-C was performed by the teacher, located in P4/4. The experiment was developed so that the students work in the laboratory session was not affected.

The objective of this experiment is to illustrate that the EDA framework can be used to detect anomalies and to identify traffic sources, in particular to perform a forensic analysis with the goal of detecting the source of the attack. The experiment is intentionally simplistic and graphics are annotated in order to simplify the interpretation of EDA for the untrained reader. Alternatively, this type of analysis could be performed using a link graph, where hosts are represented by nodes and connections are represented by edges [5]. Notice that this visualization approach is only aimed at showing interactions between hosts, and cannot be used for most other sources of data in networking. The price to pay using the EDA framework, which is context free, is that the visualization needs to be interpreted taking implicitly the context into consideration. In this example, the interpretation of the EDA tools will be performed taking the topology of the one of the three different networks, named *cell management network* in Figure 3, in mind.

In the experiment, 108 data observations were obtained with 84 variables each. After the data preprocessing to compute counter increments and remove variables with no traffic, 101 observations with 48 variables each one were left in the data set. The list of variables is included in Table 1. The 101 observations were split into a calibration group, only formed by normal traffic, and a test group, formed by both normal and Neptune attack traffic.

In Figure 4 the MEDA plot of the calibration data based on PCA is shown. Recall that the darker the value of a pair of variables m and l, the more related the features are. In the plot, it is possible to discriminate two

Table 1: SNMP variables obtained with snmpwalk in the terminals of the three switches of the cell 4.

# Var	Name	# Var	Name	# Var	Name
1	A.ifIn1	18	B.ifIn9	35	C.ifIn9
2	A.ifIn2	19	B.ifIn10	36	C.ifIn10
3	A.ifIn8	20	B.ifIn4	37	C.ifIn12
4	A.ifIn14	21	B.ifOut1	38	C.ifIn14
5	A.ifOut1	22	B.ifOut2	39	C.ifOut1
6	A.ifOut2	23	B.ifOut3	40	C.ifOut2
7	A.ifOut3	24	B.ifOut4	41	C.ifOut3
8	A.ifOut4	25	B.ifOut8	42	C.ifOut4
9	A.ifOut8	26	B.ifOut9	43	C.ifOut5
10	A.ifOut9	27	B.ifOut10	44	C.ifOut7
11	A.ifOut10	28	B.ifOut11	45	C.ifOut9
12	A.ifOut11	29	B.ifOut12	46	C.ifOut10
13	A.ifOut12	30	B.ifOut14	47	C.ifOut11
14	A.ifOut14	31	C.ifIn1	48	C.ifOut12
15	B.ifIn1	32	C.ifIn2	49	C.ifOut14
16	B.ifIn2	33	C.ifIn3		
17	B.ifIn8	34	C.ifIn5		

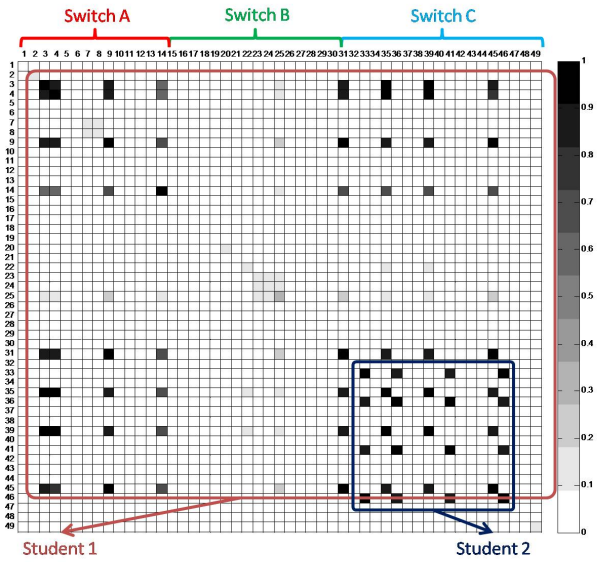

Figure 4: MEDA plot along with the two variability sources originated by the two students work.

groups of related variables highlighted in the graph. Notice that the square annotated of lowest size includes also variables of the first group which are not in the second group.

When the MEDA contains many variables, like in the present case, it may be difficult to interpret. To ease the interpretation, MEDA can be combined with a loading plot (Figure 5(a)) which shows the distribution of the variables. Loading plots are more suitable for the visualization of a high number of features. However, unlike MEDA, they are restricted to a 2-dimensional

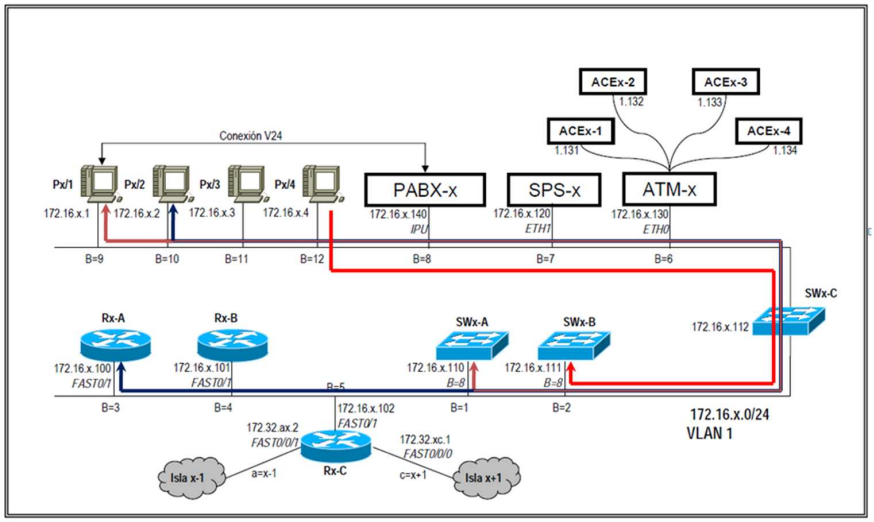

Figure 3: Network connectivity diagram in one of the three networks of the cell (management network) and traffic flow route during the work of both students (student 1 in brown and student 2 in blue) and the Neptune attack (in red). Interface n of SWx-C is represented by the text $B{=}n$ below the horizontal lines. The corresponding interfaces of switches SWx-A and SWx-B connected to SWx-C are also shown ($B{=}8$).

subspace. In a loading plot (and also in a score plot), only objects far from the origin are of interest. Variables near the origin present a low amount of variance in the subspace considered in the plot. Therefore, that subspace is not a valid choice to investigate their variability. Rather, interpretation should be focused on variables (and observations in a score plot) which are far from the origin. Also, a typical interpretation is that variables located close in a loading plot are correlated (and close observations in a score plot are similar) However, it should be noted that this is not always the case and correlation should be confirmed with MEDA. Thus, MEDA and loading plots are complementary visualization graphs which may be combined. This is also true for oMEDA and score plots.

On the other hand, to improve visualization, the MEDA matrix can also be reduced to a set of features of interest and also seriated (reordered according to a similarity criterion)[66]. The result of selecting only the features of both groups detected in Figure 4 (or the loading plot in Figure 5(a)) and obtaining the seriated (reordered) MEDA is shown in Figure 5(b).

The groups of seriated variables found with MEDA and the loading plot are listed in Table 2. A detailed analysis of these variable lets infer and trace the route followed by the network traffic in the cell, according to the network diagram of the network topology in Figure 3. The seriation performed with MEDA simplifies this task. In the first group of variables, (input and output) interfaces 8 and 14 of SW4-A are related to interfaces 1 and 9 of SW4-C. The interfaces 8 of SW4-A and 1 of SW4-C are interconnected and the interface 9 of SW4-C is connected to P4/1. Also, interface 14 of SW4-A is a virtual interface which represents VLAN1, the virtual LAN used in the configuration of the management network in Figure 3. The flow of the data can be observed in the seriated variables in Table 2: the first four interfaces are more interrelated, representing the connection from SW4-A to P4/1, while the last four represent the connection from P4/1 to SW4-A. Thus, this network traffic flow corresponds to the Telnet of student 1, between P4/1 and SW4-A. The second group of variables point to the connection of interfaces 3 and 10 of SW4-C. According to the topology, this represents the connection between P4/2 and SW4-A. Also, the incoming and outgoing flows are seen in the seriated variables. Although this is a simplistic example, it illustrates the power of MEDA to aid in the understanding of the traffic in the network.

In Figure 6(a) the score plot of the calibration data is shown. The plot shows two main directions of variability, related to two main sources of traffic. Using oMEDA, these two sources of variability can be explored. To explore the first direction of variability, towards observation 35 in the score plot, a dummy variable v_d is designed where all observations except the following are set to -1:

$$v_d(35) = 2;$$
$$v_d(37, 33, 45) = 1;$$
$$v_d(10, 2, 26, 28, 36, 6, 8, 1, 25, 14, 24, 13, 9) = 0;$$

Table 2: Groups of variables according to MEDA in Fig. 4. Each group corresponds to the Telnet traffic of each student during the session.

Group	Variables	Description
Student 1	A.ifIn14(4), C.ifIn9(35), C.ifOut1(39), A.ifIn8(3), C.ifOut9(45), A.ifOut8(9), C.ifIn1(31), A.ifOut14(14)	Telnet Configuration of Sw-A from PC-1
Student 2	C.ifOut10(46), C.ifIn3(35), C.ifOut3(41), C.ifIn10(36)	Telnet configuration of R-A from PC-2

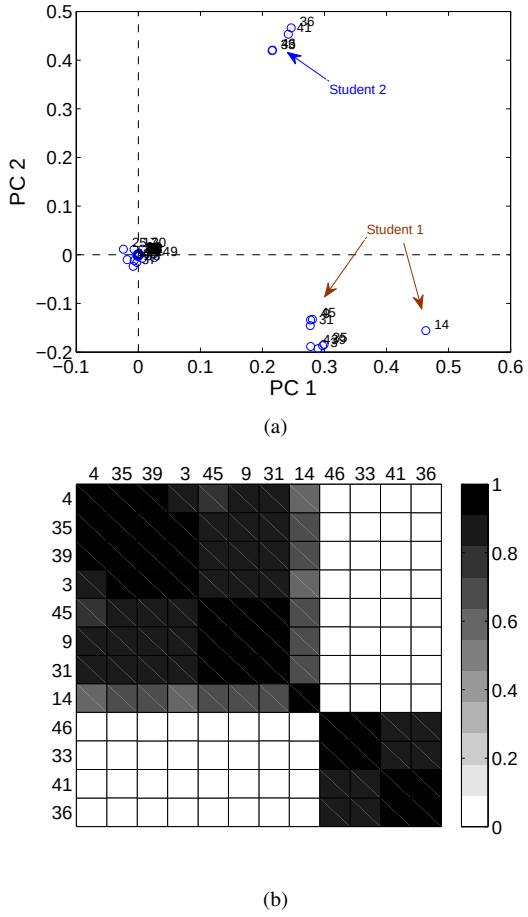

(a) (b)

Figure 5: Loading plot along with the two variability sources originated by the two students work (a) and MEDA matrix after feature selection and seriation (b).

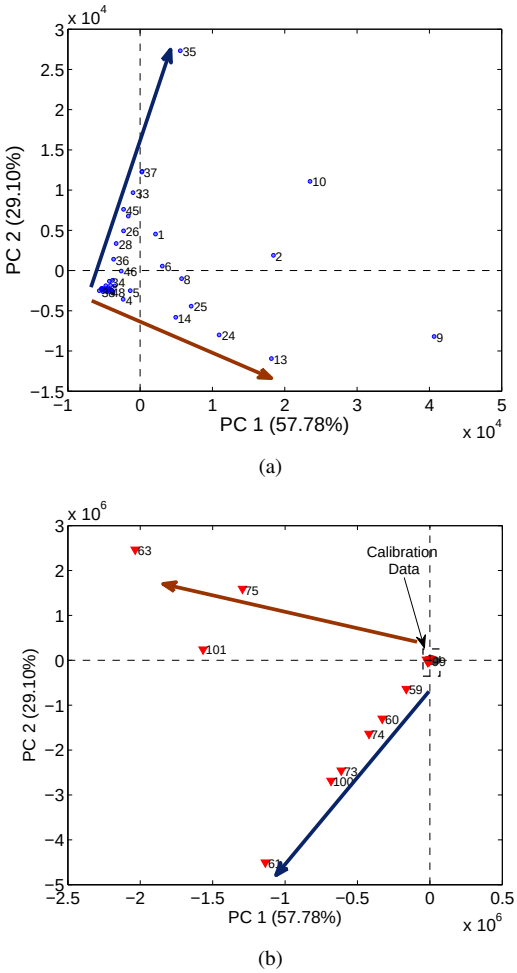

(a) (b)

Figure 6: Score plot along with the two variability sources originated by the two students work (a) and the Neptune attack (b). The area within the tiny rectangle in the origin of coordinates of (b) approximately corresponds to the area in the whole figure (a).

Thus, observations 35, 37, 33 and 45 are compared to the bulk of the data, and all the observations which are not in the direction of interest are set to zero, so that they do not contribute to the oMEDA plot. The resulting plot is shown in Figure 7(a). In this plot, the variables related to the traffic of Student 2 (recall Figure 4) are highlighted. This means that as an observation is moving towards the first direction of variability, the proportion of traffic of Student 2 is higher. Thus, observation #35 (upper left corner) represents a minute during which the traffic generated by Student 2 was especially prominent.

The second direction of variability in Figure 6(a) can be studied with the other dummy variable, where all observations are set to -1 except for:

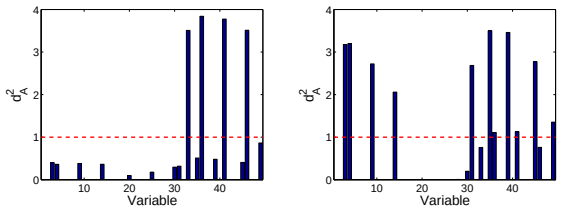

(a) (b)

Figure 7: oMEDA plots related to the direction in the score plot towards observation 35 (a) and towards 13 and 9 (b).

$$v_d(9) = 2;$$
$$v_d(13, 24) = 1;$$
$$v_d(10, 2, 26, 28, 36, 6, 8, 1, 25, 14, 35, 37, 33, 45) = 0;$$

The resulting plot is shown in Figure 7(b). Observations towards this direction have a growing amount of traffic of Student 1. Similarly, any type of pattern in the score plot, such as the particular deviation of observation 10, can be straightforwardly studied with oMEDA.

The score plot can be useful to detect anomalies in incoming traffic data. On a first phase, the projection model and score plot of normal data is obtained. Then, new incoming traffic is projected on the model and the new scores are shown in the plot in real-time. If the observations corresponding to new data are far from the calibration data, then some form of anomaly is taking place. To illustrate this, in Figure 6(b) the test observations (including the Neptune attacks) are projected on the score plot of Figure 6(a). A sub-set of the test observations are located further away from the area where the calibration data of Figure 6(a) is located. This sub-set of the test observations corresponds to Neptune attacks in the network. Simply detecting anomalous distances to the calibration data is a means to detect anomalies. The corresponding object residuals should also be inspected. This is essentially the idea beneath PCA-based anomaly detection [45, 46].

Projection models also aid in the diagnosis of the sources of the anomaly, and for this oMEDA is again useful. Thus, in Figure 6(b) two separation directions are observed: from the origin to the observation 61 and from the origin to the observation 63. The corresponding oMEDA plots for those observations are shown in Figure 8. From these plots, the reason for each deviation can be discovered. The first case corresponds to observations at the beginning of the Neptune attacks (observations 59-61, 73-74 and 100), when the packets are forwarded by SW4-C. Thus, the variables highlighted are the input interface 12 of switch C (variable 37, $C.ifIn12$), where P4/4 (the origin of the attack) is connected, and the output interface 2 of switch C (variable 20, $C.ifOut2$), where SW4-B (the destination of the attack) is connected. This plot illustrates the forensics capabilities of the analysis methods presented. The second direction of variability corresponds to the end of the transmission of the Neptune traffic (observations 63, 75 and 101) that mainly affects the input interface in SW4-B (variable #17, $B.ifIn8$). The unidirectional flow of this traffic is also illustrated in Fig. 3.

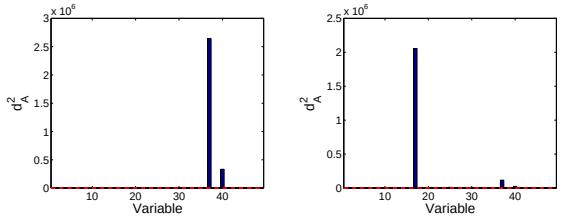

(a) (b)

Figure 8: oMEDA plots related to initial (a) and final (b) instants of the Neptune traffic.

5.2. *Connection statistic in a web page*

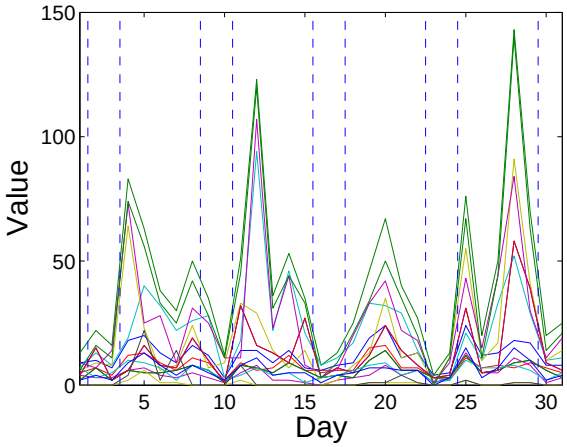

Figure 9: Time series plot of Rekom Biotech web page access data. Weekends and the rest of the week are separated using dashed lines.

In this example, the access traffic statistics of the web page of Rekom Biotech S.L. company (http://www.rekombiotech.com) collected during a month period, are analyzed using PCA. In this case, the objective is to identify the trends of access to the web and clues to increment the access of interested clients. The statistics, a total of 16, have been collected with Google Analytics © and are listed in Table 3. The data

Table 3: Traffic statistics in the collected web access.

Acronym	Description
Tv	All the visits - Visits
Tp	All the visits - Pages
UNv	New Users - Visits
UNp	New Users - Pages
VRv	Recurrent Visitors - Visits
VRp	Recurrent Visitors - Pages
TBGv	Free Traffic search engines - Visits
TBGp	Free Traffic search engines - Pages
TBv	Search traffic - Visits
TBp	Search traffic - Pages
TDv	Direct traffic - Visits
TDp	Direct traffic - Pages
TRv	Reference traffic - Visits
TRp	Reference traffic - Pages
VSRv	Visits without rebound - Visits
VSRp	Visits without rebound - Pages

set is formed by 31 observations, one per day, of 16 variables each one.

The visualization tools of Google Analytics © are limited to time series charts and pie charts, which are univariate or low-dimensional plots at best. For instance, the time series plot of the complete data set, shown in Figure 9, is not an adequate choice for visualization. Using this type of plot, only a reduced number of variables can be properly visualized. Still, the plot shows that the traffic is reduced during weekends and that there are several correlated statistics, which show a similar profile. To investigate such correlation, pairs or thirds of selected variables need to be displayed at a time. This approach is tedious and may lead to wrong conclusions, since all the possible combinations of variables are unlikely to be revised.

In Figure 10, the main visualization tools in the EDA of the web access data are shown. With only those plots, a complete picture of the data is obtained. The score plot (Fig. 10(a)) shows the distribution of the days. The use of different symbols for the days in the week is useful to detect weekly patterns. For instance, weekend days and Fridays are located towards the bottom left corner. This means that there is a different trend of access in working days and weekends. This difference can be investigated with oMEDA. The comparison with oMEDA between weekend and working days, in Fig. 10(b), shows that there is a lower amount of traffic at weekend on a general basis. This reflects the professional interest of the clients in the company. Thus, the web maintenance with down periods should be performed on weekends. The score plot also highlights especial days that are separated from the bulk of the data, for instance the case of day number 5. The traffic of any especial day can be analyzed in detail using oMEDA, in order to identify desired visiting patterns or undesired traffic to be avoided.

The MEDA plot, in Figure 10(c), is the most informative in this example. The first row or column shows that the total of visits (Tv) includes a mixture of new visitors (UNv) and recurrent visitors (VRv). This is seen in the fact that Tv is correlated to UNv and to VRv and at the same time UNv and VRv are not correlated. Thus, the total of Tv is partly UNv and partly VRv. For the same reason, Tv is a mixture of visits coming from search engines (TBGv) and direct traffic (TDv). On the other hand, the number of visited pages (Tp) is also a balanced mixture of new users (UNp) and recurrent visitors (VRp). However, direct visitors (TDp) is correlated to Tp, which reflects that this type of visitors tend to see more pages than people coming from search engines. This is also observed in the correlation of TDp and the visits without rebound (VSRp) An hypothesis on this point is that the reference words in the search engines are not totally adequate, as visitors coming from search engines seem not to be interested in the web page contents. Also, the fact that most of the incoming traffic is direct traffic and that this is partly from newcomers means that the publicity of the web url is being effective. Newcomer may find the url in the professional cards or e-mails of the company staff.

5.3. Comparative of routing algorithms in MANET

In this third example, a data-set [67] available at the CRAWDAD repository (http://crawdad.cs.dartmouth.edu/) and published in [68] is analyzed. It consists of an outdoor experiment for the comparison of three different routing algorithms in a mobile ad-hoc network (MANET) formed by 33 laptops in movement. The evaluated algorithms are:

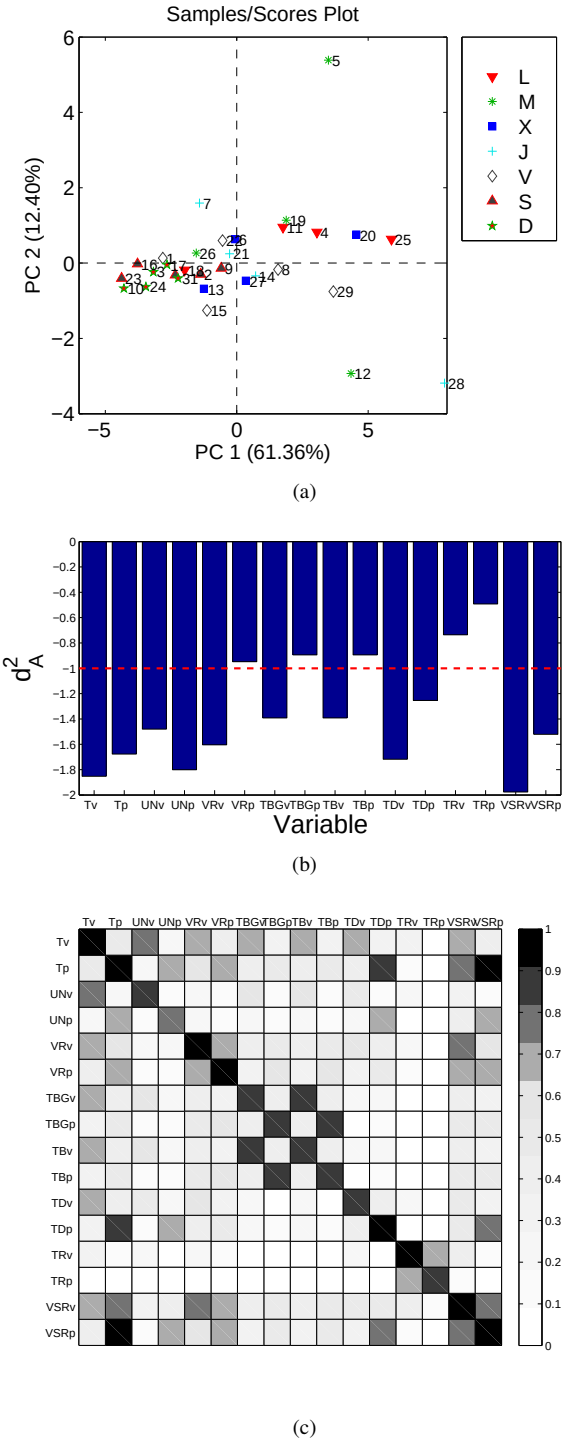

Figure 10: Visualization tools of the EDA of Rekom Biotech web page access data, using PCA: (a) score plot, (b) oMEDA plot of the difference between weekend and the rest of the week and (c) MEDA plot.

Any Path Routing without Loops (APRL), Ad hoc On-demand Distance Vector (AODV), On-Demand Multicast Routing Protocol (ODMRP) and System- and Traffic-dependent Adaptive Routing Algorithm (STARA).

The experiment was carried out in an athletics court of 225x365 meters, in which each laptop user was moving all over the field in a random manner during one hour and a half, approximately. Each laptop generated low rate traffic during this period of time. Each routing algorithm was used during 15 minutes in disjoint time intervals. The laptops positions were captured via GPS, and registered along with the number of the generated packets (TIN packets), the received ones (TOUT), or the retransmitted ones (SIN and SOUT).

The main results provided in [68] are shown in Table 4. According to the table, ODMRP is the algorithm that attains the highest message delivery ratio and STARA the one attaining the lowest: only 8% of the packets are delivered to the destination. The main reason for this low ratio is argued to be the amount of control packets generated by STARA. This is also noticed from the number of packets per message in that algorithm (second column in the table). On the other hand, AODV is the algorithm that generates the lowest amount of packets per message. Finally, ODMRP and APRL show a high hop ratio in their routes.

In this example, the EDA methodology is used to unveil more details of the experiment. For this purpose, a set of statistics listed in Table 5 are computed from the original data at regular intervals of time, yielding a total of 100 intervals. The design of these statistics is part of the EDA and should be carried out taking into account the investigation goals. Thus, the first 10 variables are related to the distribution and location of the stations (laptops) in the field, while the remaining 8 variables are related to the network traffic. This will help us determine whether some traffic differences are consequence of distribution differences. Among the 100 observations (time intervals), only those in which the four routing algorithms were active are selected (70 observations), and the rest are discarded. Thus, the final data-set is formed by 70 observations on 18 variables.

For the analysis of these data, PLS-DA is applied. The score plot, in Fig. 11, shows that the observations related to each algorithm are easily distinguished with the designed variables. This means that there are significant differences between the algorithms in the data under analysis. Notice that this fact is, by itself, a result that was not reported in Table 4, where only average values are provided with no variability analysis.

In Fig. 12, the differences between the algorithms are

Table 4: Results provided in [68].

Routing algorithm	Message delivery ratio	Packets per message	Average number of hops
AODV	0.50	7.50	1.61
APRL	0.20	33.30	2.11
ODMRP	0.77	45.59	2.47
STARA	0.08	150.67	1.18

Table 5: Considered variables.

Number	Variable	Description
1	PD	Average distance between laptops
2	mM	Minimun value for max. distances
3	Mm	Minimum value for min. distances
4	cX	X centroid X
5	cY	Y centroid Y
6	cZ	Z centroid Z
7	n1	Amount of laptops with a distance to the centroid lower than 1/32 of the max. distance
8	n2	Amount of laptops with a distance to the centroid between 1/32 and 2/32 of the max. distance
9	n3	Amount of laptops with a distance to the centroid between 2/32 and 3/32 of the max. distance
10	n4	Amount of laptops with a distance to the centroid higher than 3/32 of the max. distance
11	nTI	Number of TIN
12	nTO	Number of TOUT
13	nSI	Number of SIN
14	nSO	Number of SOUT
15	vTI	Volume of TIN
16	vTO	Volume of TOUT
17	vSI	Volume of SIN
18	vSO	Volume of SOUT

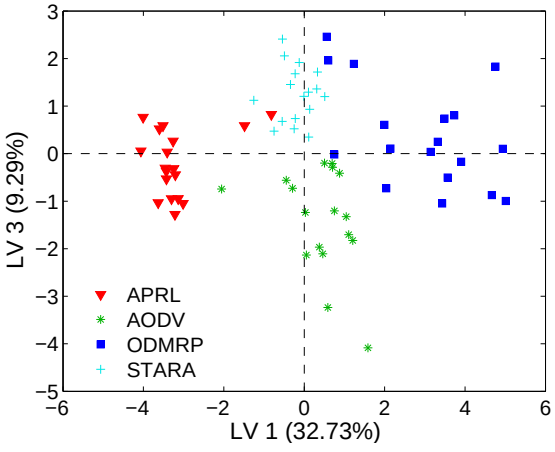

Figure 11: Score plot for the MANET experiment data.

studied with oMEDA. Fig. 12(a) provides the comparison between AODV y APRL. Surprisingly, the main differences found are related to the laptop spatial distribution and not to the routing performance. The observations corresponding to APRL present a higher dispersion in the laptop distribution, revealed by a higher value in variables PD, mM and Mm. Also, according to variables n1-n4, the number of laptops closer to the center of mass of the distribution is higher in the observations of AODV. Clearly, under these circumstances, the communication in the observations of AODV is less challenging than in the observations of APRL just because of the location of the laptops, independently of the routing algorithm used. This feature can be also observed when comparing APRL with the rest of the routing algorithms (not shown). In this situation, where the dispersion of the stations are significantly bigger for APRL, it is not possible to carry out a reliable comparison with the rest of the algorithms. Stating otherwise, the comparison is not fair because APRL is working on a more complicate scenario than its opponents. Therefore, the results provided in Table 4 for APRL must not be taken into account. This may go unnoticed if the adequate EDA tools are not used. Thus, in [68] it is mentioned that "APRL used longer routes on average than AODV". In addition, the authors state that, although ODMRP tends to emit a high number of packets, "Finally, if we consider the total number of data and control packets versus the total number of messages, we see that ODMRP surprisingly does not fare much worse than APRL". These conclusions are not adequate, considering that the working conditions for APRL are more demanding.

The oMEDA plots between AODV and ODMRP or STARA, Figures 12(b) and 12(c), also show some differences in the distribution of the nodes (e.g. n1), yet there are no differences in the global statistics of the distribution (e.g. PD). Although for an ideal comparative there should not be differences in the distribution of the laptops at all, in this case the comparison seems to be more adequate than the one including APRL. Finally, the comparison between ODMRP and STARA, presented in Figure 12(d), is under ideal conditions. In general terms, it can be seen that STARA implies a low

number of packets TOUT, what is coherent with the low message delivery ratio in Table 4. However, the differences between AODV and ODMRP regarding TOUT (or TIN) packets, in Fig. 12(b) seem not to be significant. This fact was confirmed by an adequate hypothesis test: the Welch's test (not shown). The conclusion is that the difference between the message ratio in AODV and ODMRP in Table 4 should not be understood as significant. Another element to be considered, provided by oMEDA, is the high level of retransmitted packets produced by ODMRP. This yields the high number of hops in average, in Table 4.

The clear benefit in the application of the EDA methodology in this example is the better understanding of the multivariate nature in the data. When analyzing data sets using traditional methods, the analyst needs to summarize the variables in a reduced set of statistics. This may obscure the truth underlaying the data, as it was the case in the example. The availability of powerful multivariate tools makes also possible to increment the number of variables, like we did in the example, in order to improve the investigation.

6. Conclusion

Exploratory Data Analysis (EDA) means data visualization for understanding. Once the structure of a data set is understood, it is easier to handle it adequately. EDA based on projection models is a very powerful framework to analyze complex data sets with hundreds to thousands of features. A set of recently proposed tools within this framework, revised here, simplifies the interpretation of these complex data sets.

The framework is illustrated with several small data sets. Results show that with only a few plots correctly interpreted, the user gains a detailed insight into the data, including relationships among observations, relationships among features and crossed relationships. This information, in turn, can be very informative for further data modelling, anomaly detection, diagnosis/forensics, etc.

Acknowledgments

Research in this technical report is partially supported by the Spanish Ministry of Science and Technology through grants TEC2008-06663-C03-02, TEC2011-22579 and CEI BioTIC GENIL (CEB09-0010). Dr. Pablo Padilla, Associate Professor at the University of Granada, and Dr. Jess Daz-Verdejo, Professor at the University of Granada, are gratefully acknowledged for their comments on the report.

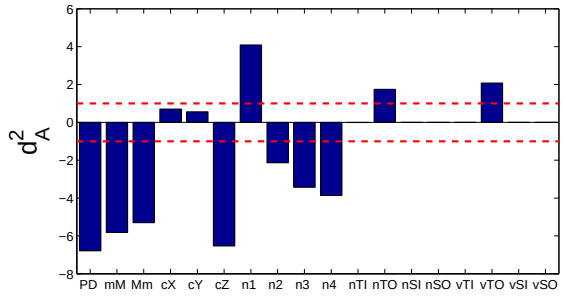

(a) AODV vs APRL

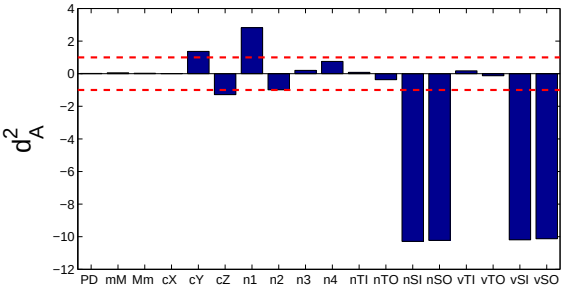

(b) AODV vs ODMRP

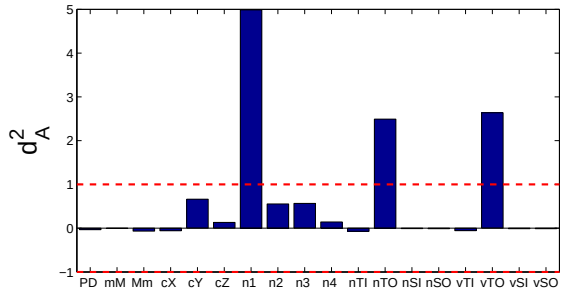

(c) AODV vs STARA

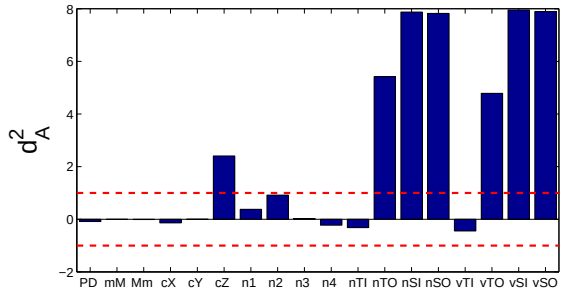

(d) ODMRP vs STARA

Figure 12: oMEDA plots for comparison between the routing algorithms.

References

[1] J. Domingo-Pascual, Y. Shavitt, S. Uhlig (Eds.), TMA'11: Proceedings of the Third international conference on Traffic monitoring and analysis, Springer-Verlag, Berlin, Heidelberg, 2011.

[2] A. Hafsaoui, G. Urvoy-Keller, D. Collange, M. Siekkinen, T. En-Najjary, Understanding the impact of the access technology: the case of web search services, in: Proceedings of the Third international conference on Traffic monitoring and analysis, TMA'11, Springer-Verlag, Berlin, Heidelberg, 2011, pp. 37–50.

[3] G. Keren, C. Lewis, A Handbook for data analysis in the behavioral sciences: statistical issues, A Handbook for Data Analysis in the Behavioral Sciences, L. Erlbaum, 1993.

[4] G. Ellis, A. Dix, A taxonomy of clutter reduction for information visualization, IEEE. Transactions on Visualization and Computer Graphics 13 (2007) 1216–1223.

[5] R. Marty, Applied Security Visualization, Pearson Education, USA, 2008.

[6] I. Jolliffe, Principal component analysis, Springer series in statistics, Springer-Verlag, 2002.

[7] J. Han, M. Kamber, Data mining: concepts and techniques, The Morgan Kaufmann series in data management systems, Elsevier, 2006.

[8] D. Ruppert, Statistics and Data Analysis for Financial Engineering, Springer Texts in Statistics, Springer, 2010.

[9] T. Yu, An exploratory data analysis method to reveal modular latent structures in high-throughput data, BMC Bioinformatics 11 (2010) 440.

[10] Y. Y. Teo, Exploratory data analysis in large-scale genetic studies, Biostatistics 11 (2010) 70–81.

[11] L. M. Sangalli, P. Secchi, S. Vantini, A. Veneziani, A case study in exploratory functional data analysis: Geometrical features of the internal carotid artery, Journal of the American Statistical Association 104 (2009) 485.

[12] K. Pearson, On lines and planes of closest fit to systems of points in space, Philosophical Magazine 2 (6) (1901) 559 572.

[13] J. Jackson, A user's guide to principal components, Wiley series in probability and mathematical statistics. Probability and mathematical statistics, Wiley-Interscience, 2003.

[14] H. Wold, E. Lyttkens, Nonlinear iterative partial least squares (NIPALS) estimation procedures, in: Bull. Intern. Statist. Inst. Proc., 37th session, London, 1969, pp. 1–15.

[15] P. Geladi, B. Kowalski, Partial least-squares regression: a tutorial, Analytica Chimica Acta 185 (1986) 1–17.

[16] S. Wold, M. Sjõstrõm, L. Eriksson, PLS-regression: a basic tool of chemometrics, Chemometrics and Intelligent Laboratory Systems 58 (2001) 109–130.

[17] J. Camacho, Missing-data theory in the context of exploratory data analysis, Chemometrics and Intelligent Laboratory Systems 103 (2010) 8–18.

[18] K. Gabriel, The biplot graphic display of matrices with application to principal component analysis, Biometrika 58 (1971) 453–467.

[19] J. Westerhuis, S. Gurden, A. Smilde, Generalized contribution plots in multivariate statistical process monitoring, Chemometrics and Intelligent Laboratory Systems 51 (2000) 95–114.

[20] J. Camacho, J. Picó, A. Ferrer, Data understanding with PCA: Structural and variance information plots, Chemometrics and Intelligent Laboratory Systems 100 (1) (2010) 48–56.

[21] P. Nelson, P. Taylor, J. MacGregor, Missing data methods in PCA and PLS: score calculations with incomplete observations, Chemometrics and Intelligent Laboratory Systems 35 (1996) 45–65.

[22] F. Arteaga, A. Ferrer, Dealing with missing data in MSPC: several methods, different interpretations, some examples, Journal of Chemometrics 16 (2002) 408–418.

[23] F. Arteaga, A. Ferrer, Framework for regression-based missing data imputation methods in on-line MSPC, Journal of Chemometrics 19 (2005) 439–447.

[24] I. V. Mechelen, A. Smilde, A generic linked-mode decomposition model for data fusion, Chemometrics and Intelligent Laboratory Systems 104 (2010) 83–94.

[25] A. Smilde, J. Westerhuis, S. de Jong, A framework for sequential multiblock component methods, Journal of Chemometrics 17 (2003) 323–337.

[26] F. Lindgren, B. Hansen, W. Karcher, M. Sjõstrõm, L. Eriksson, Model validation by permutation tests: Applications to variable selection, Journal of Chemometrics 10 (1996) 521–532.

[27] S. Wiklund, D. Nilsson, L. Eriksson, M. Sjõstrõm, S. Wold, K. Faber, A randomization test for PLS component selection, Journal of Chemometrics 21 (2007) 427–439.

[28] N. Faber, R. Rajkó, How to avoid over-fitting in multivariate calibration–the conventional validation approach and an alternative, Analytica Chimica Acta 595 (2007) 98–106.

[29] A. Kassidas, J. MacGregor, P. Taylor, Synchronization of batch trajectories using dynamic time warping, AIChE Journal 44 (1998) 864–875.

[30] N. Nielsen, J. Carstensen, J. Smedsgaard, Aligning of single and multiple wavelength chromatographic profiles for chemometrics data analysis using correlation optimised warping, Journal of Chromatography 805 (1998) 17–35.

[31] J. González-Martnez, A. Ferrer, J. Westerhuis, Real-time synchronization of batch trajectories for on-line multivariate statistical process control using dynamic time warping, Chemometrics and Intelligent Laboratory Systems 105 (2011) 195–206.

[32] R. Bro, A. Smilde, Centering and scaling in component analysis., Journal of Chemometrics. 17 (2003) 16–33.

[33] J. Camacho, Exploratory Data Analysis using latent subspace models., INTECH, 2012.

[34] J. Camacho, Observation-based missing data methods for exploratory data analysis to unveil the connection between observations and variables in latent subspace models, Journal of Chemometrics 25 (11) (2011) 592–600.

[35] Traffic Monitoring and Analysis (TMA), `http://www.tma-portal.es`.

[36] Traffic Analysis and Classification (TRAC), `http://netserv.iet.unipi.it/trac2012`.

[37] Large Scale Network Analysis (LSNA), `http://www.largenetwork.org/`.

[38] Internet Measurement Conference (IMC), `http://www.sigcomm.org/events/imc-conference`.

[39] C. M. Burns, J. Kuo, S. Ng, Ecological interface design: a new approach for visualizing network management, Comput. Netw. 43 (3) (2003) 369–388.

[40] Q. Liao, A. Blaich, D. VanBruggen, A. Striegel, Managing networks through context: Graph visualization and exploration, Computer Networks 54 (16) (2010) 2809 – 2824.

[41] D. Phan, J. Gerth, M. Lee, A. Paepcke, T. Winograd, Visual analysis of network flow data with timelines and event plots., in: J. R. Goodall, G. J. Conti, K.-L. Ma (Eds.), VizSEC, Mathematics and Visualization, Springer, pp. 85–99.

[42] D. S. Shelley, M. H. Gunes, Gerbilsphere: Inner sphere network visualization, Computer Networks 56 (3) (2012) 1016 – 1028.

[43] V. Chatzigiannakis, S. Papavassiliou, G. Androulidakis, Improving network anomaly detection effectiveness via an integrated multi-metric-multi-link (m3l) pca-based approach, Security and Communication Networks 2 (3) (2009) 289–304.

[44] G. Mnz, Traffic Anomaly Detection and Cause Identification Using Flow-Level Measurements. PhD thesis, Technische Uni-

versitt Mnchen, 2010.

[45] D. Brauckhoff, K. Salamatian, M. May, Applying pca for traffic anomaly detection: Problems and solutions, in: INFOCOM 2009. 28th IEEE International Conference on Computer Communications, Joint Conference of the IEEE Computer and Communications Societies, 19-25 April 2009, Rio de Janeiro, Brazil, IEEE, 2009, pp. 2866–2870.

[46] H. Ringberg, A. Soule, J. Rexford, C. Diot, Sensitivity of pca for traffic anomaly detection, SIGMETRICS Perform. Eval. Rev. 35 (1) (2007) 109–120.

[47] P. Minarik, T. Dymacek, Netflow data visualization based on graphs, in: Proceedings of the 5th international workshop on Visualization for Computer Security, VizSec '08, Springer-Verlag, Berlin, Heidelberg, 2008, pp. 144–151.

[48] D. Rolls, G. Michailidis, F. Hernández-Campos, Queueing analysis of network traffic: methodology and visualization tools, Computer Networks 48 (3) (2005) 447 – 473.

[49] E. Acar, B. Yener, Unsupervised multiway data analysis: A literature survey, IEEE Transactions on Knowledge and Data Engineering 21 (2009) 6–20.

[50] L. Bernaille, R. Teixeira, K. Salamatian, Early application identification, in: Proceedings of the 2006 ACM CoNEXT conference, CoNEXT '06, ACM, New York, NY, USA, 2006, pp. 6:1–6:12.

[51] C. Dhanjal, S. Gunn, J. Shawe-Taylor, Efficient sparse kernel feature extraction based on partial least squares, IEEE Transactions on Pattern Analysis and Machine Intelligence 31 (2009) 1347–1361.

[52] S. Wold, Cross-validatory estimation of the number of components in factor and principal components, Technometrics 20 (4) (1978) 397–405.

[53] J. Camacho, A. Ferrer, Cross-validation in PCA models with the element-wise k-fold (EKF) algorithm: Teoretical aspects, Submitted to Journal of Chemometrics.

[54] Y. Song, F. Nie, C. Zhang, S. Xiang, A unified framework for semi-supervised dimensionality reduction, Pattern Recognition 41 (2008) 2789–2799.

[55] X. Zhao, Y. Liu, Generative tracking of 3D human motion by hierarchical annealed genetic algorithm, Pattern Recognition 41 (2008) 2470–2483.

[56] E. Alaa, D. Hasan, Face recognition system based on pca and feedforward neural networks, in: J. Cabestany, A. Prieto, F. S. Hernández (Eds.), Lecture notes in computer science, ISSN 0302-9743, Vol. 3512 of Lecture Notes in Computer Science, Springer, 2005, pp. 935–942.

[57] H. He, X. Yu, A comparison of PCA/ICA for data preprocessing in remote sensing imagery classification, in: D. Li, H. Ma (Eds.), MIPPR 2005: Image Analysis Techniques, Proceedings of the SPIE, Volume 6044, 2005, pp. 60–65.

[58] T. Kourti, J. MacGregor, Multivariate SPC methods for process and product monitoring, Journal of Quality Technology 28 (4) (1996) 409–428.

[59] A. Ferrer, Multivariate statistical process control based on principal component analysis (MSPC-PCA): Some reflections and a case study in an autobody assembly process, Quality Engineering 19 (4) (2007) 311–325.

[60] M. Barker, W. Rayens, Partial least squares for discrimination, Journal of Chemometrics 17 (2003) 166–173.

[61] T. Nguyen, G. Armitage, A survey of techniques for internet traffic classification using machine learning, Communications Surveys Tutorials, IEEE 10 (4) (2008) 56 –76.

[62] J. Camacho, P. Padilla, J. Díaz-Verdejo, Least-squares approximation of a space distribution for a given covariance and latent sub-space, Chemometrics and Intelligent Laboratory Systems 105 (2) (2011) 171 – 180.

[63] F. Lindgren, B. Hansen, W. Karcher, M. Sjstrm, L. Eriksson, Model validation by permutation tests: Applications to variable selection, Journal of Chemometrics 10 (5-6) (1996) 521–532.

[64] S. Wiklund, D. Nilsson, L. Eriksson, M. Sjstrm, S. Wold, K. Faber, A randomization test for PLS component selection, Journal of Chemometrics 21 (10-11) (2007) 427–439.

[65] Network forensic frameworks: Survey and research challenges, Digital Investigation 7 (12) (2010) 14 – 27.

[66] G. Caraux, S. Pinloche, Permutmatrix: a graphical environment to arrange gene expression profiles in optimal linear order.

[67] R. S. Gray, D. Kotz, C. Newport, N. Dubrovsky, A. Fiske, J. Liu, C. Masone, S. McGrath, Y. Yuan, CRAWDAD data set dartmouth/outdoor (v. 2006-11-06), Downloaded from http://crawdad.cs.dartmouth.edu/dartmouth/outdoor (Nov. 2006).

[68] R. S. Gray, D. Kotz, C. Newport, N. Dubrovsky, A. Fiske, J. Liu, C. Masone, S. McGrath, Y. Yuan, Outdoor experimental comparison of four ad hoc routing algorithms, in: Proceedings of the 7th ACM international symposium on Modeling, analysis and simulation of wireless and mobile systems, MSWiM '04, 2004, pp. 220–229.